Experimental investigation of 3D-printed tubular and swirl star grains as solid fuels for hybrid rocket engines

M El-Naggar[1*], Ahmed Farid Ayad[2], and Anwer Hashish[3]

[1] PhD student, Aerospace Engineering Department, Military Technical College, Egypt

[2] Associate Professor, Aerospace Engineering Department, Military Technical College, Egypt

[3] Associate Professor, Aerospace Engineering Department, Military Technical College, Egypt

*E-mail: msmnajjar89@gmail.com

Abstract. This study investigates using 3D-printed Acrylonitrile Butadiene Styrene (ABS) polymers as fuels for hybrid rocket engines through 27 static fire experiments. It evaluates the performance of ABS fuel grains across various motor sizes and compares the effects of direct and swirl injection in ABS/G_{ox} hybrid engines. Regression rate relations with oxidizer mass flux are established for three configurations: a modified one-inch motor with ABS fuel tubular grain and swirl star grain with the modified motor. The swirl injection enhances the mixing and combustion efficiency, leading to increased regression rates. This research highlights the advantages of swirl injection in optimizing hybrid rocket performance and contributes to advancements in hybrid rocket technology. To enhance the fuel regression rate of hybrid rockets, a solid fuel grain featuring a star swirl reverse port was 3D printed using ABS fuel, with G_{ox} as the oxidizer. Tests of the engine's combustion with this grain indicated that, at a constant oxidizer mass flow rate, the star-swirl reverse improved both thrust and specific impulse compared to tubular and traditional circular port grains.

1. Introduction

The primary objective of hybrid rocket motors (HREs) is to leverage the combined advantages of solid and liquid propulsion systems, offering a balance of performance that combines the safety and simplicity of solid rockets with the throttling and restart capabilities of liquid rockets. HRE stands positioned between its two rivals and finally, Figure 1 provides an overview of the hybrid rocket engine (HRE) system. A typical HRE includes a tank for storing the oxidizer, which can be in liquid or gaseous form, a single propellant feed system, and a combustion chamber containing the solid fuel grain. Offering cost-effective and environmentally friendly propulsion, HRE advantages include safer handling, lower production costs, and adaptability to various applications. However, low fuel regression rates, combustion inefficiencies, and thrust instabilities have limited their usage. Advancements in fuel formulations, grain geometries, and manufacturing technologies are addressing these issues, making hybrid rocket motors increasingly viable for modern aerospace applications [1, 2]. Since no single HRE design is ideal for every application, rocket scientists need to understand the system features, maximize its strengths, and mitigate its weaknesses to create a propulsion system that meets specific mission requirements [3].

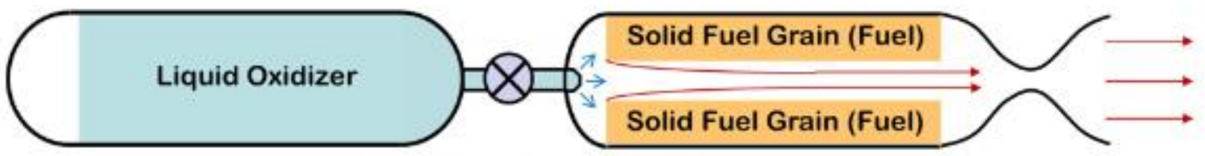

Figure 1. Sketch of a Hybrid rocket propulsion architecture [3]

Unlike solid rocket motors, the regression rate of hybrid fuel grain depends on the oxidizer mass flux and chemical characteristics of both oxidizer and fuel. The regression rate equation is identified as follows:

$$r = aG_{ox}^{n} \tag{1}$$

where r is the fuel regression rate (mm/s)

a is an empirical constant depends on fuel composition, oxidizer, and motor condition

n is an empirical exponent (between 0.5 and 0.8)

G_{ox} is an oxidizer mass flux and equal $(\mathrm{kg/m^2.s})$

$$G_{ox} = \frac{\dot{m}_{ox}}{A_p} \tag{2}$$

where $\dot{m}_{ox}$ is an oxidizer mass flow rate. (kg/s)

A_p is a port cross-sectional area of the grain (mm^2), which is the internal burning surface area where the oxidizer flows through the solid fuel grain.

To enhance the regression rate of hybrid rocket engines, researchers used different techniques i) The use of multi-port grain geometries [4] ii) use of liquifying fuels [5, 6] iii) use of swirl injectors[4, 5, 7–9] iv) use of unconventional motors [5, 7]

Paravan et.al [5] showed that 3D-Printing offers variable grain geometries that are hard to manufacture using casting techniques. complex shapes can be easily produced including swirling of the port to enhance vortex flow inside the motor. Several studies have been made to maximize the gain of these new manufacturing techniques in terms of increasing the regression rate of hybrid rocket engines. The key factor to improve the regression rate is the heat transfer dynamics inside the motor to enhance the thermal conductivity and combustion efficiency.

Olsen, et.al [10] examined the effect of copper-enhanced 3D-printed ABS fuel grains on hybrid rocket motor performance. Using additive manufacturing, ABS was infused with varying copper concentrations (2%, 4%, and 6%) to enhance thermal conductivity and fuel regression rates. Results demonstrated a moderate increase in regression rates with copper addition, improving propellant density and volumetric efficiency while maintaining combustion stability.

Solid fuel grains with a star-fractal swirl port geometry were introduced in [11, 12] as shown in Figure 2 to enhance fuel regression rates. The grains were produced using 3D-Printer. The star fractal as shown in the figure design was created by sweeping while rotating axially at a constant pitch This trade-off highlights the balance between manufacturing efficiency and optimal performance in propulsion system development. These combined studies confirm that the star-fractal swirl port significantly enhances the regression rate of hybrid rocket fuel grains compared to conventional circular and star-fractal ports. Combustion experiments showed increased thrust and specific impulse, with fuel surface regression occurring more rapidly at concave sections of the star-fractal geometry, leading to enhanced thrust and specific impulse. The successful launch of a hybrid rocket incorporating this design achieved a record altitude of 10.1 km, demonstrating its practical effectiveness.

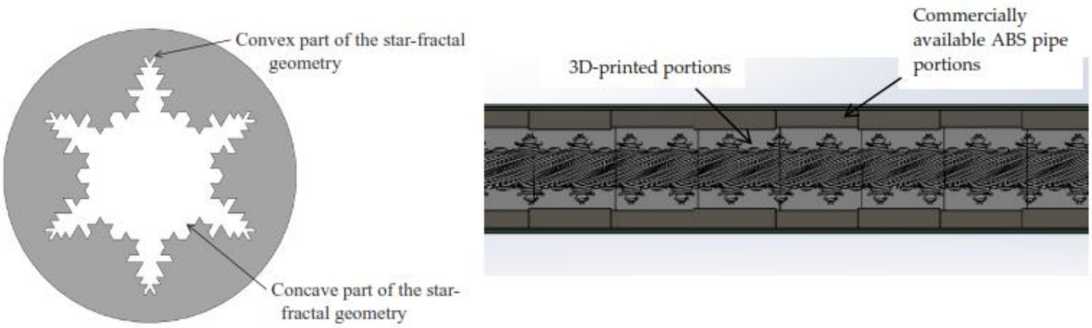

Figure 2. The geometry of swirl star-fractal used in [11, 12]

Wang et.al [9] presented the design and testing of a swirl-radial-injection composite fuel grain for hybrid rocket engines. The innovative grain, composed of 3D-printed ABS and paraffin-based fuel, enhanced oxidizer-fuel mixing through helical swirl blades, improving combustion efficiency and regression rates. Experimental results showed that the swirl-radial design significantly increases fuel regression rates compared to traditional front-end injection systems while reducing front-end ablation. As shown in Figure 3, the swirl-radial-injection fuel combines a 3D-printed ABS substrate with paraffin-based fuel to enhance combustion in hybrid rocket engines. The ABS structure, featuring integrated spiral blades, ensures uniform radial oxidizer injection and induces swirling flow, improving fuel-oxidizer mixing and combustion efficiency.

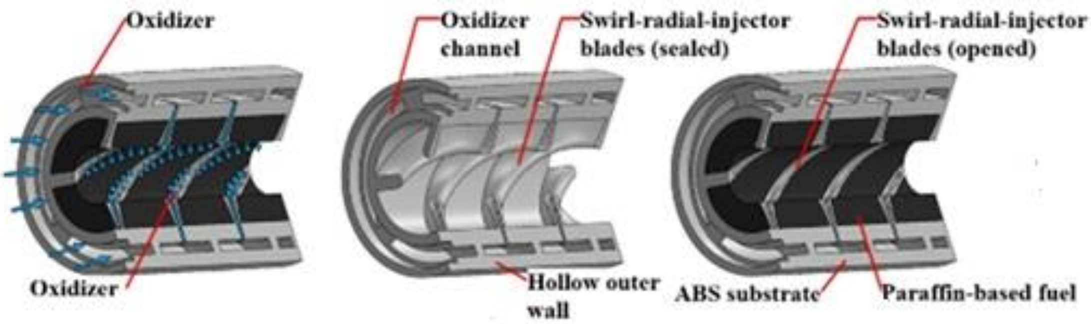

Figure 3. The swirl radial injectors' cross-sections [9]

Armold, et.al [13] demonstrated the potential of rapid prototyping in fabricating hybrid rocket fuel grains with complex swirl patterns including acrylic straight port, swirl star acrylic port, swirl star filled with paraffin, and straight port paraffin acrylic. Experiment results confirm that 3D-printed acrylic and paraffin fuel grains, combined with swirl-inducing geometries, can achieve up to a 270% increase in regression rates. In comparison, cast paraffin with aluminum additives shows a 70% improvement. Additionally, an oxidizer swirl injection was found to enhance burn efficiency further in cast paraffin samples.

The lack of a rich database about hybrid rocket engines in the open literature is the prime driver of the present experimental study. The research activity has been done in two phases. In the first phase, tubular fuel grain is investigated along with oxygen with different pre and post-combustion chamber dimensions. In the second phase, star swirl counter flow fuel grain is investigated with a swirl injector using the motor that gives the most stable burning. The remainder of the paper is organized as follows. The following section illustrates the aspects of the case study solid fuel grain. Next, Aspects of experiments and design of experiments (DOE) are explained. Discussion of results follows and the paper concludes with the key findings.

2. Case study and experimental methodology

2.1 Solid fuel grain

The choice of ABS as fuel is based on many reasons which include low cost, and availability, ABS can be easily modified with additives, such as metal powders or energetic compounds, to enhance its combustion characteristics. ABS processes unique burn characteristics when burned with gaseous oxygen. Finally, ABS is more environmentally friendly than other fuel materials, as it produces fewer hazardous emissions during combustion. ABS formula is $C_{3.85}H_{4.85}N_{0.43}$

where Acrylonitrile (43%), Butadiene (50%), and Styrene (7%) and it's heat of formation 62.63J.

Two types of grains were used in this study. The reverse swirl is 7-star as shown in Figure 4 while the tubular grain with different port areas as shown in Figure 5.

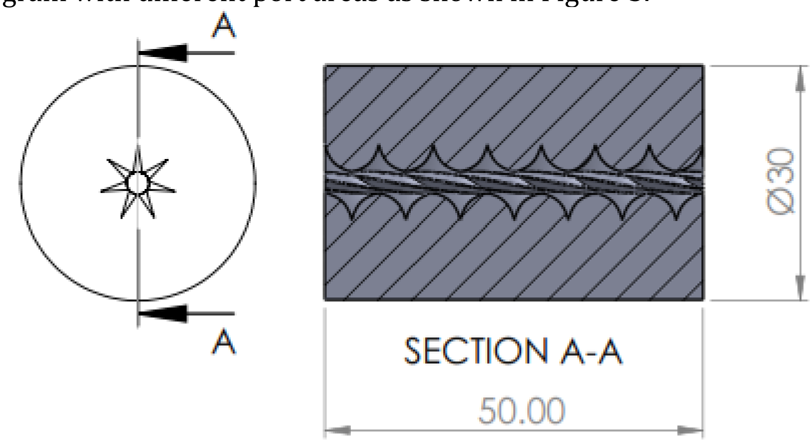

Figure 4 Reverse swirl star grain

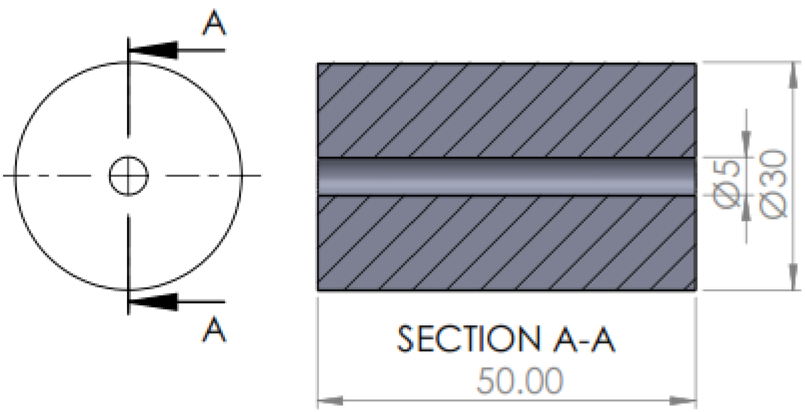

Figure 5 Tubular grain

The fuel grains are fabricated using a 3D-printed ABS filament. A Prusa i3 MK3 printer was employed for this process. The grain settings during the generation of the G_code for 3d printing are indicated in Table 1. Once printed, the grains are inserted in a metal case as illustrated in Figure 6.

Table 1. 3D Printing setting and grain dimension

Parameter	Description
Infill	100%
Filament	Prusa ABS
layer height	0.15 mm
Nozzle Temperature	230°C
Bed Temperature	105°C
Material density	943 g/cm^3
Lamination pitch	0.254 mm
Modeling method	Sparse printing
Grain outer diameter	30 mm
Grain length	50 mm
Port length	2.8 mm
Port cross-section area	949 mm^2

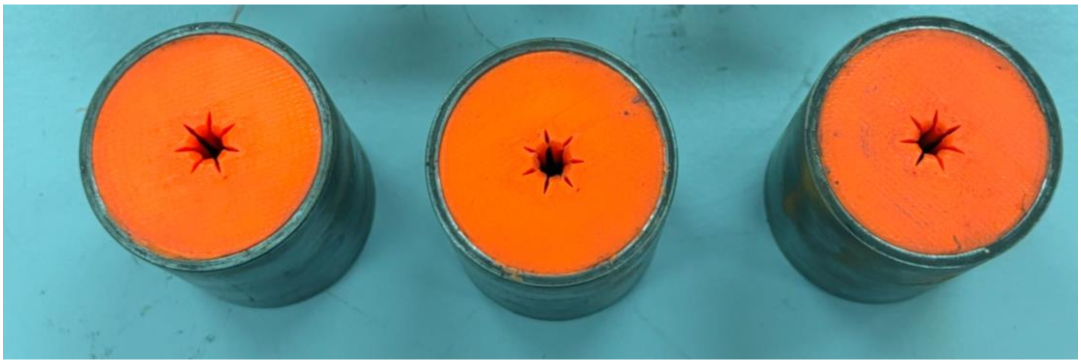

Figure 6. Reverse swirl star after 3d printing and insertion in metal case

2.2 Test motors

Figure 7 shows the 1-inch motor originally designed for solid grain testing and converted is adapted for hybrid testing. The head features an injection port compatible with various injector types (swirl, showerhead, etc.) and a separate port for pressure measurement using a pressure transducer. The impact of pre- and post-combustion chambers is sought. This is planned by using two motors namely, the long and the modified one-inch motors both handling the same grain. Lengths of pre- and post-combustion chambers are 15 mm and 28 mm, respectively, 90.5 mm and 82 for the modified motor, respectively, for the long motor. The nozzle throat is 5 mm in diameter for both diameters.

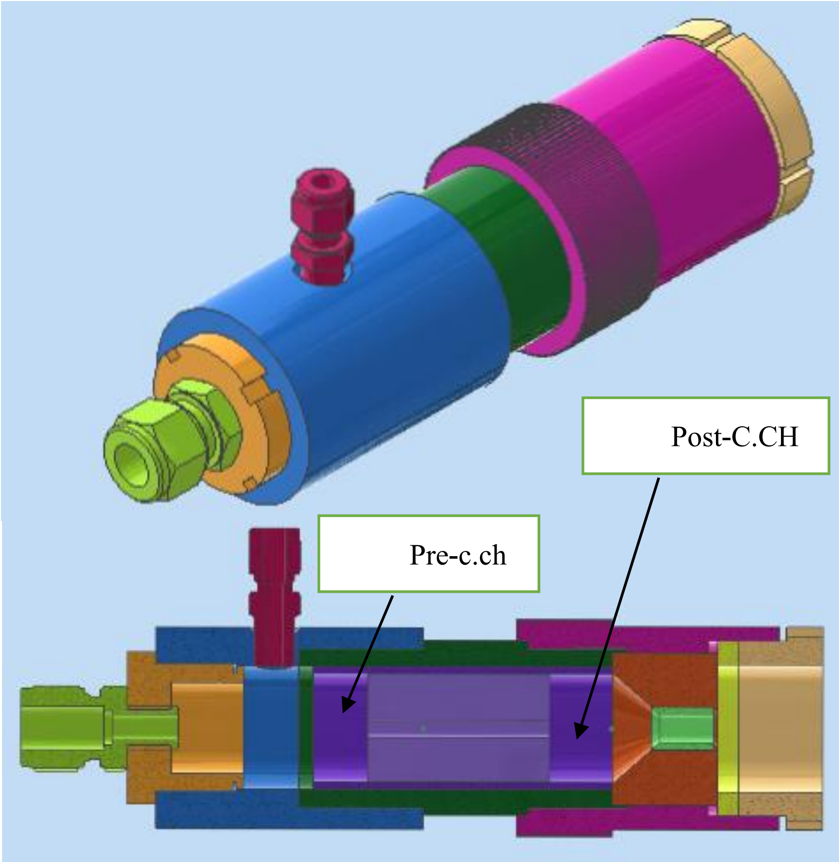

Figure 7. The one-inch test motor

To guarantee a suitable range of the oxidizer-to-fuel (O/F) ratio throughout the operation, an oxidizer mass flow rate of 5 g/s was chosen. This selection considers the anticipated increase in burning area as the fuel grain regresses. Swirl injectors are shown in Figure 8 They introduce a tangential component to the oxidizer flow during injection. This creates a swirling motion within the combustion chamber, potentially leading to several benefits compared to traditional direct injection.

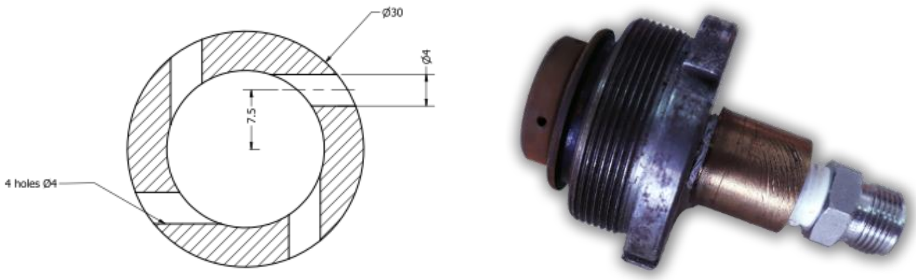

Figure 8. Swirl injector

2.3 Test setup

The schematic shown in Figure 9 illustrates the preparation of a 1-inch motor and shows that the oxidizer tank holds the used oxidizer G_{ox}. Nitrogen is utilized for immediate cooling after shutdown to ensure that ignition is halted. By following the piping, one can see how the gases pass through valves and flow control elements until they reach the combustion chamber.

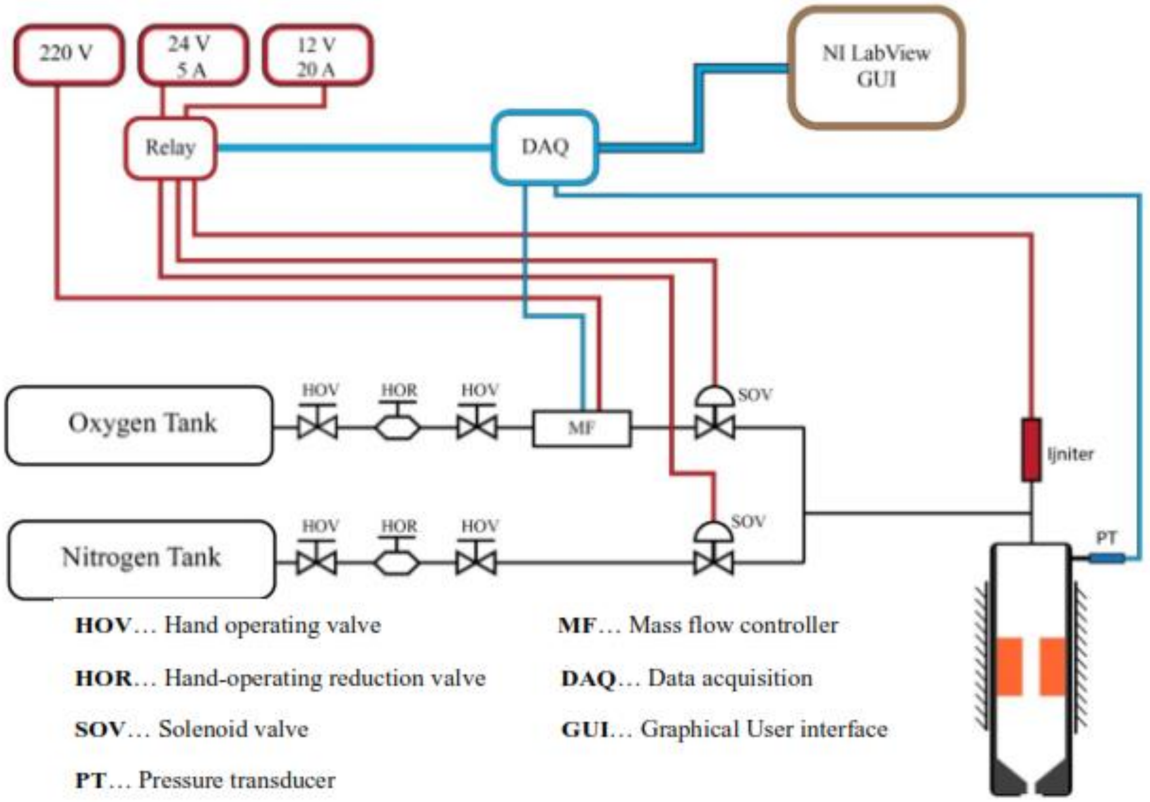

Figure 9. Test setup preparation

Ignition is achieved using a small solid propellant charge composed of HTPB (hydroxyl-terminated polybutadiene) and AP (ammonium perchlorate). This charge is heated to ignition by the Joule effect in a Kanthal wire wrapped around the arms of the igniter. The current flow through the wire, upon circuit closure, generates heat, which subsequently ignites the propellant charge.

2.4 Data reduction

The goal of these tests is to determine the correlation between the oxidizer mass flux (G_{ox}) and the fuel regression rate (r). The coefficients, denoted as a and n, equation (1) are derived from the curve-fitting process. The regression rate is assumed to be uniform along the motor axis.

The average combustion chamber pressure can be calculated as follows:

$$p_{avg} = \frac{1}{t_b}\int_{\Delta t_b} p_c(t)\,dt \tag{3}$$

The regression rate is calculated using the equation

$$r = \frac{(\Delta m_f)}{\rho \overline{A_b} t} \tag{4}$$

$$\Delta m_{grain(f)} = m_{grain\,(i)} - m_{grain\,(f)} \tag{5}$$

Where ρ is the propellant density (g/cm^3), $m_{grain\,(i)}$ *and* $m_{grain\,(f)}$ are the initial and final grain mass (kg), t is the burning time (sec) and A_b is the burning area of the grain (mm^2)

On the other hand, the oxidizer mass flux is expressed as

$$G_{ox} = \frac{\dot{m}_{ox}}{\overline{A_P}} \tag{6}$$

The sum of initial and final port areas of the grain is

$$\overline{A_P} = \frac{A_{P,i}+A_{P,f}}{2} \tag{7}$$

2.5 Test matrix

Experiments are designed to address the two factors in concern namely, grain design and motor size. According to equation (3), the regression rate depends on operating time. Hence, three burn time values are examined. As shown in Table 2, 9 types of experiments are designed. Each experiment is repeated 3 times yielding a total of 27 firing.

Table 2 Test matrix for the firing experiments

Exp designation	t (sec)	Modified one-inch motor		Long one-inch motor
		Tubular grain	Swirl star grain	Tubular grain
R1:R3	4	3 firings	3 firings	3 firings
R4:R6	7	3 firings	3 firings	3 firings
R7:R9	10	3 firings	3 firings	3 firings

3. Results & Discussion

3.1 Results for tubular fuel grains:

The table below summarizes all pre- and post-firing data of tubular grains in a modified one-inch motor, considering an oxidizer mass flow rate of approximately 5 g/s and ABS density of 943 kg/m^3.

Table 3. Results of measurement for a modified 1-inch motor with Swirl Injection tubular ABS fuel grain

EXP NO	t sec	m_i gram	m_f gram	l_i mm	l_f mm	D_i mm	D_f mm	r_f mm/s	G_{ox} kg/m^2.s
R1	3.81	105.7	100.3	50.12	46.4	4.65	11.24	1.39	100.8
R2	3.63	107.4	100.2	50.02	46.58	4.65	10.95	1.38	104.6
R3	3.66	107.3	100.8	49.76	46.12	4.65	11.01	1.42	103.7
R4	6.83	108.4	91.4	50	44.25	4.65	14.51	1.13	69.3
R5	6.80	105.4	94.4	50.07	43.59	4.65	15.72	1.10	61.3
R6	6.81	105.1	98.1	49.73	43.25	4.65	14.25	1.11	71.2
R7	9.72	108	92	50.07	41.42	4.65	16.97	0.91	54.4

R8	9.53	107.7	92.8	49.8	40.06	4.65	17.8	0.89	52.4
R9	9.72	108.8	92	49.87	39.47	4.65	7.981	0.91	49.7

In contrast, the table below lists the corresponding data for tubular grain in long one-inch motor.

Table 4. Results of measurement for a modified 1-inch motor with Swirl Injection tubular ABS fuel grain

EXP NO	t sec	m_i gram	m_f gram	l_i mm	l_f mm	D_i mm	D_f mm	r_f mm/s	G_{ox} $kg/m^2.s$
R1	4.52	109.9	101.9	49.77	45.91	4.73	12.10	1.42	89.78
R2	4.94	110	102.1	50.17	46.48	4.78	12.01	1.28	90.25
R3	4.82	109.7	101.8	50.18	46.84	4.84	11.7	1.33	92.90
R4	4.89	101.9	95.4	45.9	38.26	12.10	16.68	0.67	30.72
R5	4.89	102.1	94.	46.48	38.43	12.01	17.2	0.73	29.84
R6	4.23	101.8	94.3	46.84	38.67	11.7	17.01	0.88	30.85
R7	4.26	110	98.5	50.23	44.46	4.77	15.08	1.82	103.31
R8	5.17	110.4	97.6	50.18	43.32	4.71	15.83	1.62	96.45
R9	4.39	109.5	98.8	50.20	44.55	4.74	14.63	1.69	108.42

3.2 Results for reversed swirl star fuel grains:

The resultant data of the reverse swirl star grain in a modified one-inch motor is described in Table 5.

Table 5. Results of measurement for 1-inch motor with swirl injection ABS-swirl star

EXP NO	t sec	m_i gram	m_f gram	l_i mm	l_f mm	D_i mm	D_f mm	r_f mm/s	G_{ox} $kg/m^2.s$
R1	3.86	105.7	97	50	46.84	4.65	13.8	1.63	74.3
R2	3.86	107.4	98.6	50	46.26	4.65	14.05	1.64	72.7
R3	3.9	107.3	98.3	50	46.74	4.65	14.5	1.61	69.4
R4	6.84	108.4	95.2	50	43.09	4.65	16.7	1.22	55.57
R5	6.87	105.4	91.9	50	44.4	4.65	18	1.16	49.3
R6	6.89	105.1	91.3	50	43.99	4.65	18.17	1.17	48.9
R7	9.89	108	90.4	50	40.8	4.65	20.8	0.94	39.18
R8	9.88	107.7	89.7	50	41.2	4.65	19.3	1.02	44.32

R9	9.89	108.8	91	50	40.8	4.65	19.85	0.98	42.39

The fuel grain performance was analyzed under various conditions, including swirl injection methods for long and modified one-inch motors. This analysis produced detailed regression rate laws for each scenario, indicating that the reversed star-swirl grain significantly enhanced the regression rate compared to the tubular grain using the modified one-inch motor, as shown in. Figure 10. The regression rate coefficients are calculated numerically using the test data and are summarized in Table 6. Regression rate coefficients. This improvement is due to better mixing and increased combustion efficiency from the turbulent flow created by the swirl mechanism. Swirl injection in both long and modified one-inch motor configurations resulted in higher regression rates, demonstrating its effectiveness across different motor sizes. In the case of tubular grains, the modified one-inch motor shows a slower regression rate compared to the original one but in terms of stability, the modified motor shows better stability.

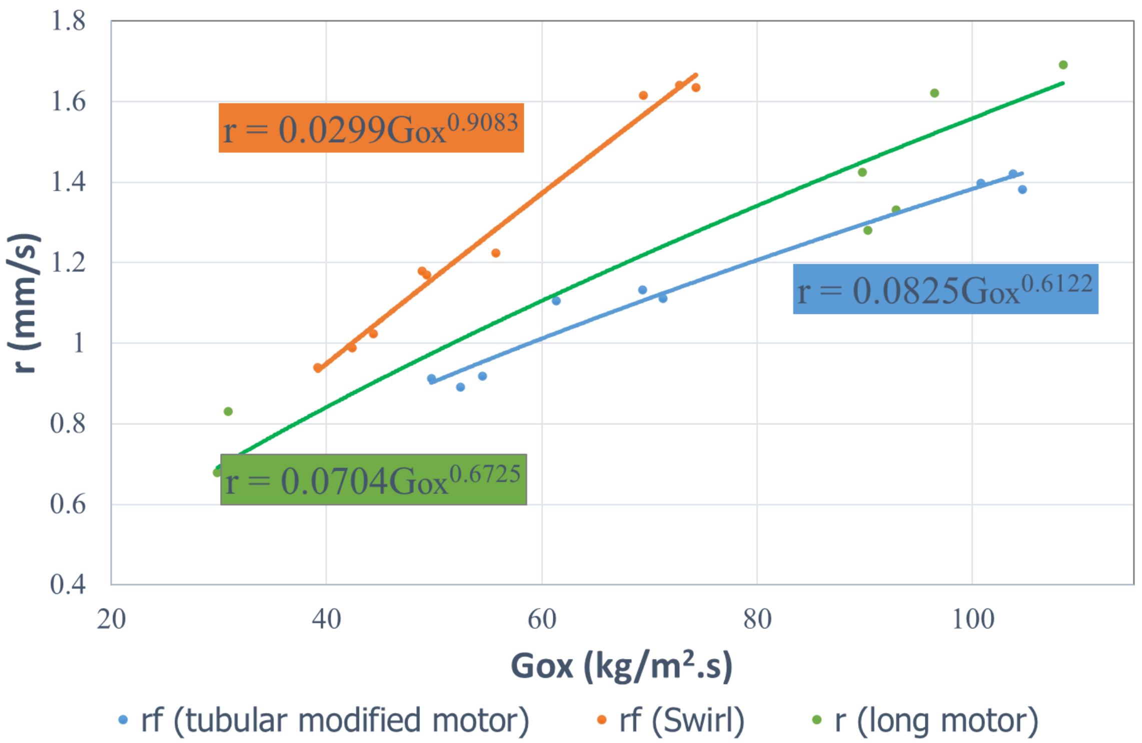

Figure 10. Regression Rate Laws of Different Conditions

Table 6. Regression rate coefficients

Coefficient	Modified one-inch motor		Long one-inch motor
	Tubular grain	Swirl star grain	Tubular grain
a	0.0825	0.0704	0.0299
n	0.6122	0.6725	0.9083

4. Conclusion

The turbulence of tubular grain with swirl injectors in the original one-inch motor has more instability although slightly high regression rates. But when using a modified motor, the stability is better than the old motor and an enhancement in instabilities of the tubular swirl injector in the modified one-inch motor caused to decrease in the regression rate using a reverse swirling star (new curve) with high vortices, the turbulence reduced instability causing to increased the regression rate and the combustion efficiency So, the regression rate for swirl star is better than tubular for long and modified one-inch motors.

Acknowledgment

The authors would like to thank Prof. Mahmoud Y M Ahmed for his valuable contributions in conducting the project and preparing this paper.

References

[1] Wei S-S, Li M-C, Lai A, et al. A Review of Recent Developments in Hybrid Rocket Propulsion and Its Applications. Aerospace 2024; 11: 739.

[2] Mane S. Advancements in hybrid rocket motor technology: Safety, performance, and applications. Int J Enhanc Res Sci Technol Eng,2023.

[3] Altman D. Hybrid rocket development history. In: 27th Joint Propulsion Conference. 1991, p. 2515.

[4] Therese Jens E. Hybrid Rocket Propulsion Design Handbook. Academic Press, 2023.

[5] Paravan C, Galfetti L, Bisin R, et al. Combustion Processes in Hybrid Rockets. International Journal of Energetic Materials and Chemical Propulsion.

[6] Oztan C, Ginzburg E, Akin M, et al. 3D printed ABS/paraffin hybrid rocket fuels with carbon dots for superior combustion performance. Combust Flame 2021; 225: 428–434.

[7] Santolini V, Paravan C. Innovative Methodology for Evaluating Combustion Efficiency in Swirled Rocket Engines. In: 75 th International Astronautical Congress (IAC). 2024, pp. 14–18.

[8] Stella M, Zeni L, Nichelini L, et al. Experimental Investigation of a H2O2 Hybrid Rocket with Different Swirl Injections and Fuels. Applied Sciences (Switzerland); 14. Epub ahead of print 1 July 2024. DOI: 10.3390/app14135625.

[9] Wang R, Lin X, Wang Z, et al. Combustion Characteristics of a Swirl-Radial-Injection Composite Fuel Grain with Applications in Hybrid Rockets. Aerospace; 10. Epub ahead of print 1 September 2023. DOI: 10.3390/aerospace10090759.

[10] Olsen KC, Forester P, Whitmore SA, et al. Test and Evaluation of Copper-Enhanced, 3-D Printed ABS Hybrid Rocket Fuels. In: AIAA Propulsion and Energy 2021 Forum. 2021.

[11] Funami Y, Takano A. Regression-Rate Evaluation of Hybrid-Rocket Fuel Grain with a Star-Fractal Swirl Port. Trans Jpn Soc Aeronaut Space Sci 2023; 66: 61–69.

[12] Takano A, Yoshino K, Fukushima Y, et al. System Design and Launch of a Hybrid Rocket with a Star-Fractal Swirl Fuel Grain Toward an Altitude of 15 km †. Applied Sciences (Switzerland); 14. Epub ahead of print 1 December 2024. DOI: 10.3390/app142311297.

[13] Armold D, Boyer JE, Kuo KK, et al. Test of hybrid rocket fuel grains with swirl patterns fabricated using rapid prototyping technology. In: 49th AIAA/ASME/SAE/ASEE Joint Propulsion Conference. American Institute of Aeronautics and Astronautics Inc., 2013. Epub ahead of print 2013. DOI: 10.2514/6.2013-4141.